Journal of Science and Transport Technology
Journal homepage: https://jstt.vn/index.php/en

UNIVERSITY OF TRANSPORT TECHNOLOGY

Influence of Cross-Sectional Configuration on the Dynamic Response of High-Speed Railway Bridges

Khanh Nguyen[1], Le Hung Tran[2], Thang Ba Phung[3,*]
[1]Escuela Técnica Superior de Ingeniería Aeronáutica y del Espacio, UPM, Madrid, Spain
[2]Université Gustave Eiffel, France
[3]Faculty of Civil Engineering, University of Transport Technology, Hanoi, Vietnam

Article info
Type of article:
Original research paper

DOI:
https://doi.org/10.58845/jstt.utt.2026.en.6.3.196-215

[*]**Corresponding author:**
Email address:
thangpb@utt.edu.vn

Received: 31/03/2026
Received in Revised Form: 29/06/2026
Accepted: 15/07/2026

Abstract: This study investigates the effect of cross-sectional configuration and skewness on the dynamic response of short-span, high-speed railway bridges. Three-dimensional finite element models were developed for the following four 30 m simply supported bridge configurations: I-girder, U-girder, hollow slab and box girder. To enable a controlled comparison, the following parameters were maintained consistently across the investigated cases: span length, deck depth, material properties, support idealisation, track position and HSLM-A1 loading scheme. A single train load was applied along an eccentrically positioned track to activate vertical bending and torsional responses. The first vertical bending frequencies of the straight bridges were closely grouped between 4.63 Hz and 4.67 Hz. However, their speed-dependent responses differed substantially, indicating that the fundamental bending frequency alone is insufficient to explain the dynamic behaviour of bridge decks with different structural configurations. The hollow slab bridge exhibited the lowest response levels over the investigated speed range, whereas the I-girder bridge showed the greatest variation between the centre of the bridge and the position of the loaded track. This behaviour was associated with the proximity of the bending and torsional modes under eccentric loading. As the skew angle increased from 0° to 40°, the hollow slab bridge showed the greatest increase in the first vertical bending frequency (approximately 22.5%), while the I-girder bridge showed only a slight increase (approximately 1.5%). In this study, the resonance formula based on the fundamental bending frequency is used as a reference estimate for straight bridges, rather than as a complete predictor of the response of skew bridge decks. The results show that the effect of skewness depends on the configuration and is governed by the combined effects of modal characteristics, transverse stiffness distribution, torsional response and support geometry. These findings are specific to the adopted moving-load model and provide evidence to inform the selection of an appropriate analytical level in the preliminary dynamic assessment of high-speed railway bridges.

Keywords: High-speed railway bridge; cross-sectional configuration; torsional stiffness; bending–torsion coupling; skew angle; resonance velocity; finite element modelling.

1. Introduction

In recent decades, high-speed railway (HSR) systems have developed rapidly worldwide and have become one of the most efficient and sustainable modes of transportation. Owing to their advantages in terms of energy efficiency, high passenger transport capacity, and reduced greenhouse gas emissions, HSR has been increasingly adopted by many countries as a key solution for regional and intercity transportation [1, 2].

In high-speed railway lines, bridges, particularly viaducts, constitute a significant proportion of both the number of structures and the total route length. This is mainly due to the stringent geometric requirements of high-speed railway alignments, including large curve radius, small longitudinal gradients, and high track straightness to ensure operational safety and dynamic stability when trains run at high speeds. In addition, the use of bridges helps to reduce track settlement and subgrade deformation, minimize level crossings, facilitate the crossing of complex terrain, and mitigate environmental impacts and land acquisition requirements. According to the pre-feasibility study report of the North–South high-speed railway project in Vietnam, the total length of bridges and viaducts accounts for a large proportion of the overall route length [3]. A similar trend has also been observed in many high-speed railway systems worldwide, where bridge structures typically account for approximately 40% to more than 70% of the total line length [4, 5].

In high-speed railway bridges, the dynamic behaviour of the structure is a key factor that directly affects operational safety, the long-term durability of the structure, and passenger comfort. When trains travel at high speeds, the dynamic loads acting on the bridge may induce significant vibrations and may even lead to resonance if the train speed coincides with the natural frequency of the structure. Therefore, modern railway bridge design standards impose stringent requirements regarding the dynamic analysis of bridges, including the verification of natural frequencies, limits on displacement and acceleration, and the evaluation of train–bridge interaction to ensure operational safety and running stability at high speeds [6–9].

The cross-sectional configuration has a direct influence on the fundamental stiffness characteristics of the structure, particularly the bending and torsional stiffness. Closed cross-sections, such as box sections, generally exhibit significantly higher torsional stiffness than open sections such as I- or T-girders. This difference arises from the shear stress transfer mechanism in thin-walled closed sections, which enables the cross-section to resist torsional deformation more effectively. In contrast, the bending stiffness of a member is strongly governed by the moment of inertia of the cross-section [10–12]. The dynamic behaviour of a structure is primarily governed by its stiffness, mass distribution, and damping characteristics. These factors determine the natural frequencies, mode shapes, and the potential for resonance under dynamic loading [13, 14].

For high-speed railway bridges, moving train loads at high speeds may excite structural vibration modes and, in some cases, lead to dynamic resonance when the train speed approaches or coincides with the natural frequency of the bridge [15]. The dynamic behaviour of railway bridges becomes more complex due to the interaction among the moving train, the bridge structure, and the track system. In certain situations, the bending and torsional vibration modes of the structure may also be coupled under moving train loads [16–19].

In practice, bridge structures in general, and railway bridges in particular, especially reinforced concrete bridges with short and medium spans, can be designed with various types of cross-sections. Common configurations include I-beam, U-beam, hollow slab, and box girder. Each cross-sectional type possesses distinct characteristics in terms of load-carrying capacity, material efficiency, and dynamic performance. The selection of these cross-sections generally depends on the span length, construction conditions, and the technical requirements of the railway line (Fig. 1) [20, 21].

Previous studies have examined the dynamic response of individual railway bridges to trains, including those with steel–concrete composite box girders, locally deformed bridge decks and skew configurations [22], [23], [24], [25], [26]. These studies suggest that the dynamic behaviour of railway bridges cannot be fully understood by considering only the first vertical bending frequency. In particular, the distribution of torsional stiffness, transverse load transfer, support geometry and modal interaction may be important when the train load is eccentric or the bridge is skewed. However, direct comparison between bridge typologies remains difficult because cross-sectional configuration commonly changes alongside span length, deck depth, structural mass, support arrangement and loading conditions. Consequently, the reported differences in dynamic response cannot always be attributed to the configuration of the bridge itself. Therefore, a controlled numerical comparison is required to distinguish the response characteristics associated with I-girder, U-girder, hollow slab and box-girder bridge decks under a common structural and loading framework.

This study is a comparative numerical investigation rather than a project-specific design or optimisation exercise. Four bridge configurations are examined using three-dimensional finite element models under the same span length, deck depth, material properties, support idealisation, track eccentricity and HSLM-A1 moving-load scheme. The study addresses three questions: (i) How does cross-sectional configuration modify the modal properties and speed-dependent responses of high-speed railway bridges? (ii) How does the response differ between the bridge centreline and the loaded-track position under eccentric loading? (iii) How does the resonance behaviour of each bridge configuration change with skew angle? The study's contribution lies in establishing a configuration-based interpretation of dynamic response, rather than ranking bridge types as universally superior or inferior. The results aim to clarify the circumstances in which the first bending frequency can be used as a preliminary indicator, and the situations in which three-dimensional effects associated with torsional response, transverse stiffness distribution and skew support geometry need to be considered explicitly.

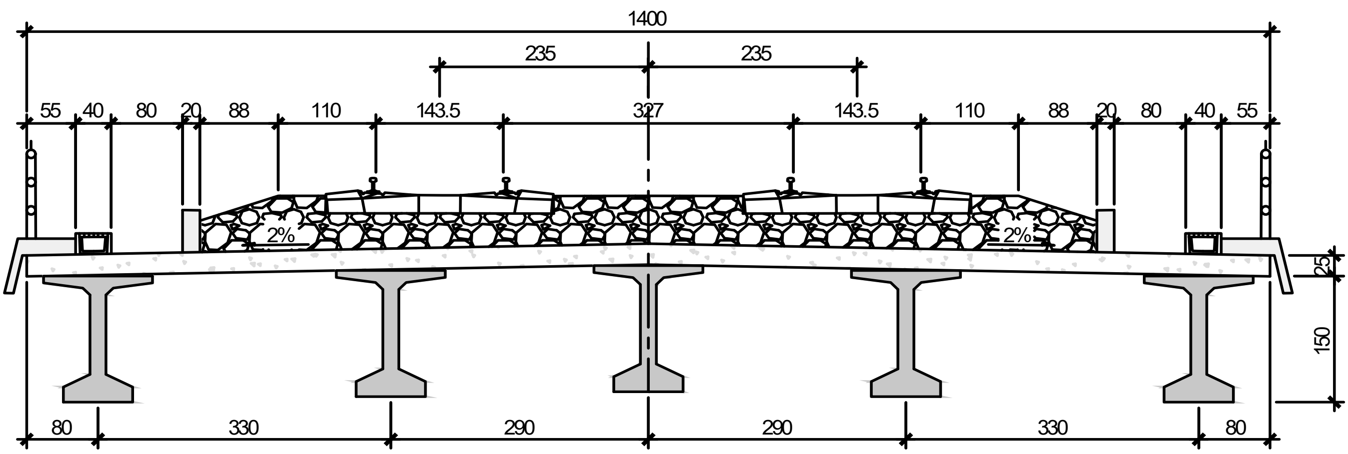

(a) I-beam deck section

Fig. 1. Typical cross-sectional configurations used in high-speed railway bridges

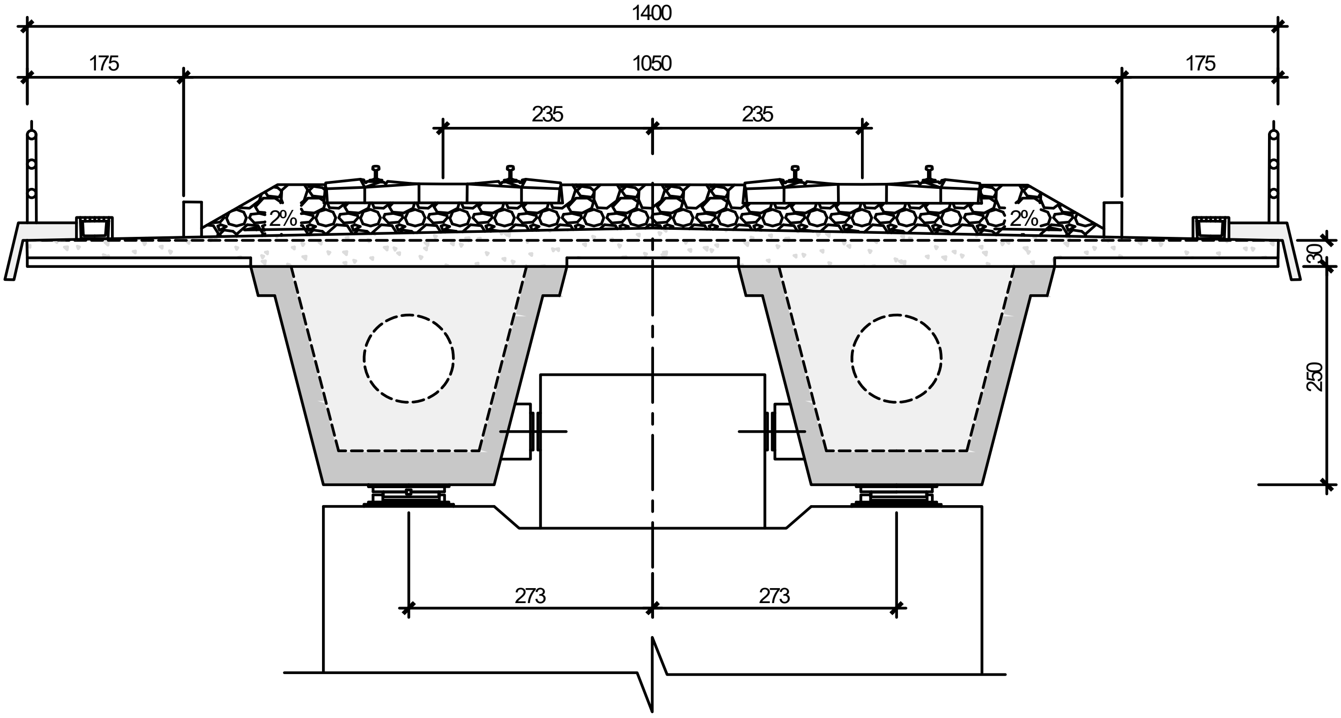

(b) U-beam deck section

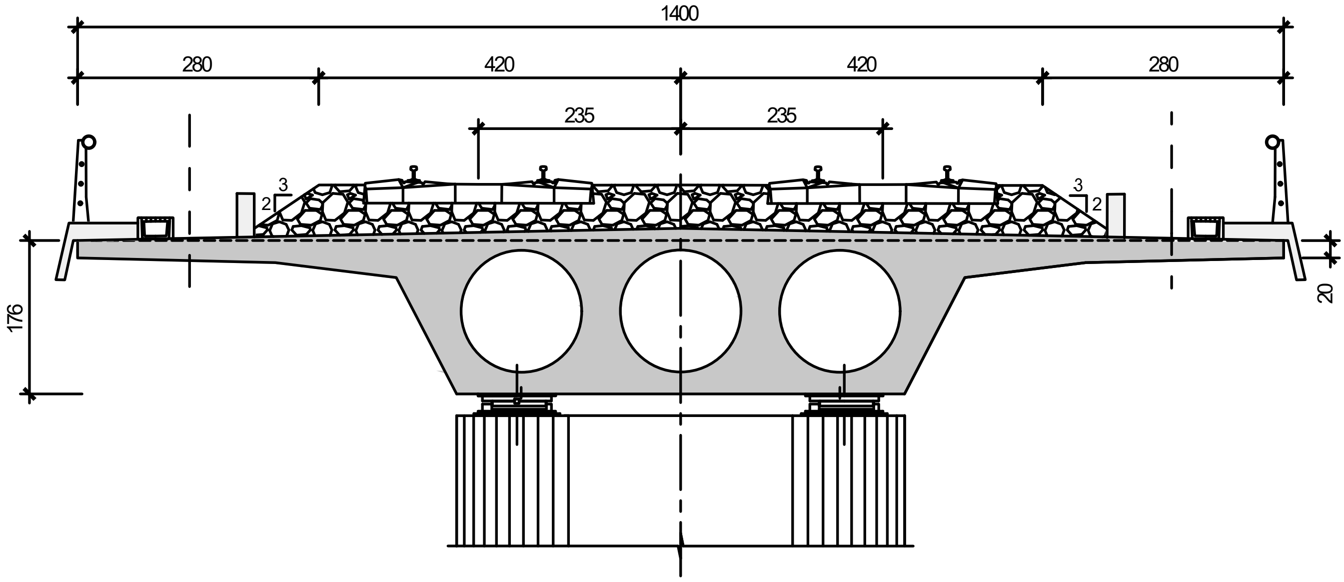

(c) Hollow slab deck section

Fig. 1. (continued)

2. Numerical Framework and Comparative Modelling Strategy

2.1. Moving-load model

In railway bridge dynamics, three levels of idealisation are commonly used: the moving-load model, the moving-mass model, and the moving-suspension-mass model [15], [18]. This study uses the moving-load idealisation (see Fig. 2) because the aim is to compare the dynamic behaviour of bridge decks under an identical excitation scheme for different configurations, rather than to reproduce the complete train–track–bridge interaction of a specific bridge. Consequently, the same HSLM-A1 axle sequence, loading path, speed range and eccentric track position are applied to all bridge configurations. This modelling approach excludes vehicle suspension, wheel–rail contact, track irregularity and track load-spreading effects. These mechanisms may be relevant for operational safety assessments or detailed analyses of train–bridge interactions. However, the moving-load approach provides a transparent and computationally efficient basis for parametric and comparative investigations, provided that the conclusions are confined to the adopted loading model [27], [28]. The moving HSLM-A1 load was generated using a Python routine to construct the time-dependent nodal load vector (F(t)) for each prescribed train speed. This routine maintains consistent axle spacing, axle sequence, loading path, temporal discretisation and load-transfer procedure across all bridge configurations. This ensures that any differences in the computed responses originate from the bridge models rather than from inconsistencies in the moving-load definition.

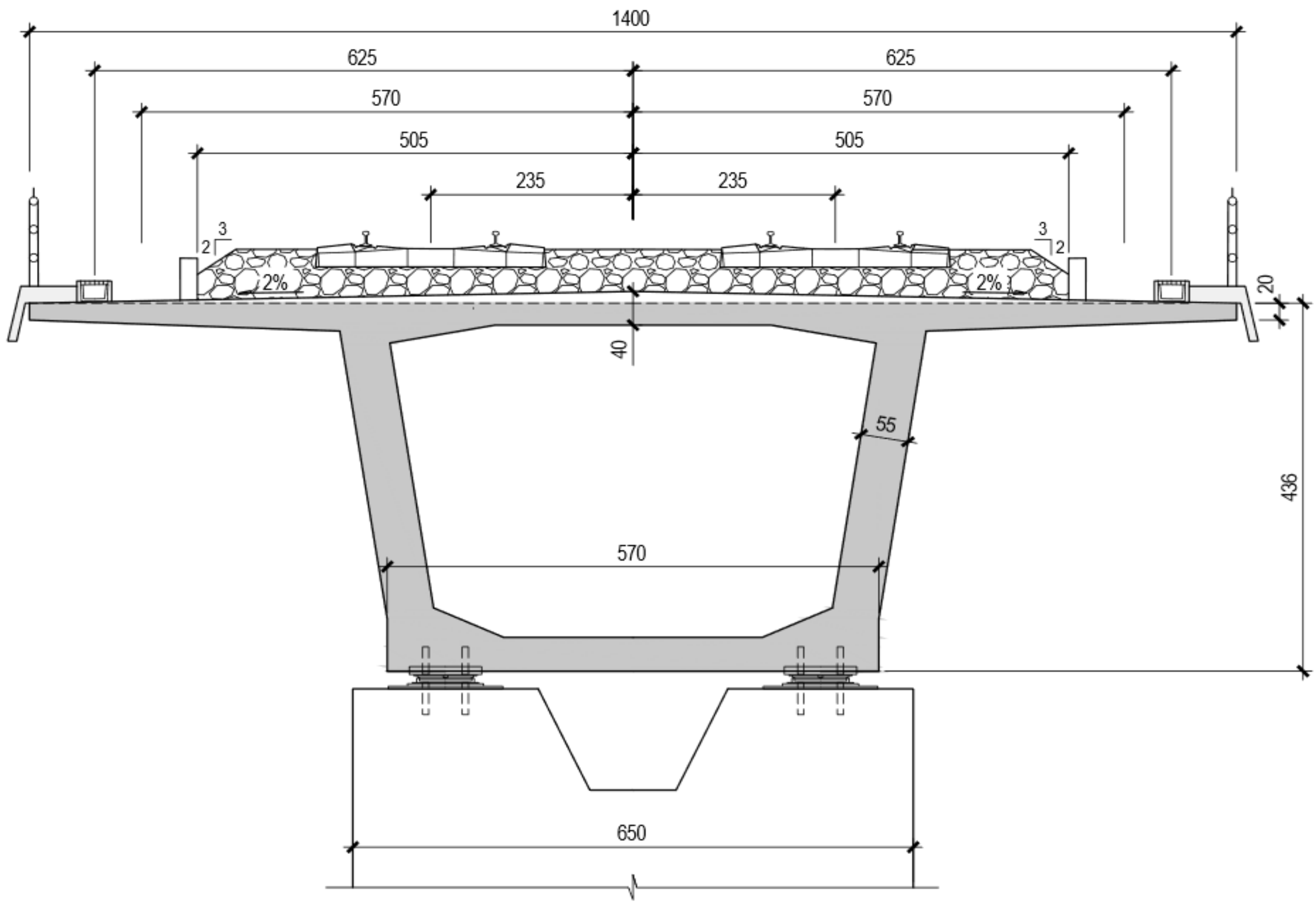

(d) Box girder deck section

Fig. 1. (continued)

2.2. Bridge model

The bridge structure is modelled using the finite element method (FEM), employing a combination of beam, shell and solid elements. The equations of motion for a bridge subjected to a train travelling at a constant velocity v can be expressed as:

$$\mathbf{M\ddot{X}+C\dot{X}+KX=F} \quad (1)$$

where **M**, **C** and **K** are the mass, damping, and stiffness matrices of the bridge system and F is the nodal forces vector due to the train loads.

2.3. Numerical solution procedure

To solve Eq. (1) in the time domain, the modal superposition technique is adopted. The bridge response is represented as a linear combination of mode shapes and their corresponding modal coordinates, resulting in a set of uncoupled equations expressed in terms of the generalized modal coordinates. Depending on the bridge configuration, support conditions and skew angle, the natural frequencies and associated mode shapes are first determined numerically [29]. The resulting uncoupled equations are subsequently integrated in the time domain using the piecewise exact method [14].

2.4. Comparative modelling basis, response measures and study scope

The numerical programme was designed as a controlled comparative study to investigate how bridge cross-sectional configuration affects the dynamic response when subjected to a standard loading framework. The four bridge models were defined with identical span lengths, nominal deck depths, material properties, support idealisation, track arrangement, HSLM-A1 loading schemes, train speed ranges and nominal mesh sizes. These common conditions were adopted to ensure that any observed differences in response could primarily be attributed to the structural configuration of the deck system.

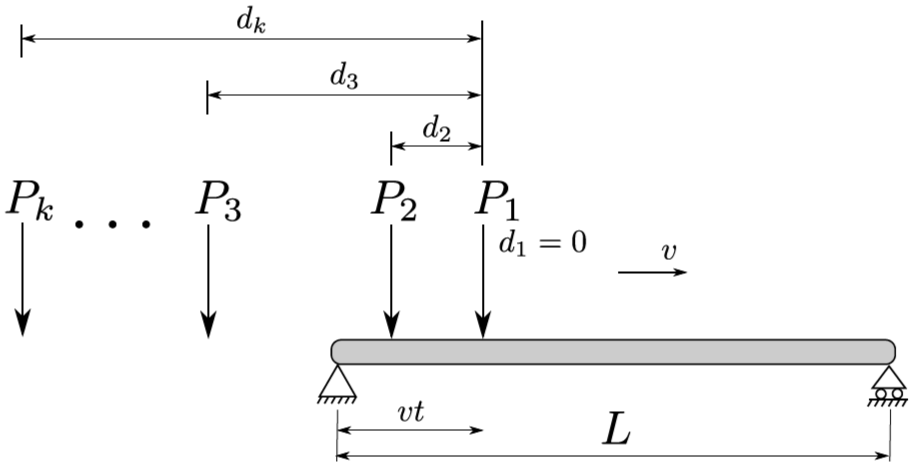

Fig. 2. Train model as a convoy of moving loads

The bridge configurations were not artificially adjusted to have identical mass, flexural stiffness, transverse stiffness or torsional stiffness. These properties are an inherent consequence of the adopted cross-sectional layouts and form part of the structural characteristics being compared. Accordingly, the present analysis does not attempt to isolate the independent contribution of a single parameter, such as torsional stiffness. Instead, the combined configuration-dependent effects of mass and stiffness distribution, cross-sectional continuity, and the load-transfer mechanism on the global dynamic response are evaluated. For each bridge configuration, the response was evaluated at two locations: the bridge centreline (denoted CDT) and the loaded-track position (denoted CDV). At each train speed, the peak vertical displacement and peak vertical acceleration were extracted at both locations. The response envelopes obtained over the investigated speed range were then used to identify the principal resonance region, compare the spatial variation of the response across the deck width and assess the influence of the skew angle on the response magnitude and resonance velocity.

The study focuses on linear-elastic, simply supported bridge models with a 30 m span length, subjected to a single HSLM-A1 moving load acting on an eccentrically located track. Vehicle suspension, wheel–rail contact, track irregularity, train–track–bridge interaction and local stress responses are beyond the scope of this study. Therefore, the findings should be interpreted as comparative evidence based on configuration for preliminary dynamic modelling, rather than as a complete assessment of a specific bridge or full verification of running safety.

3. Comparative Bridge Configurations

3.1. Bridge configurations and three-dimensional finite element models

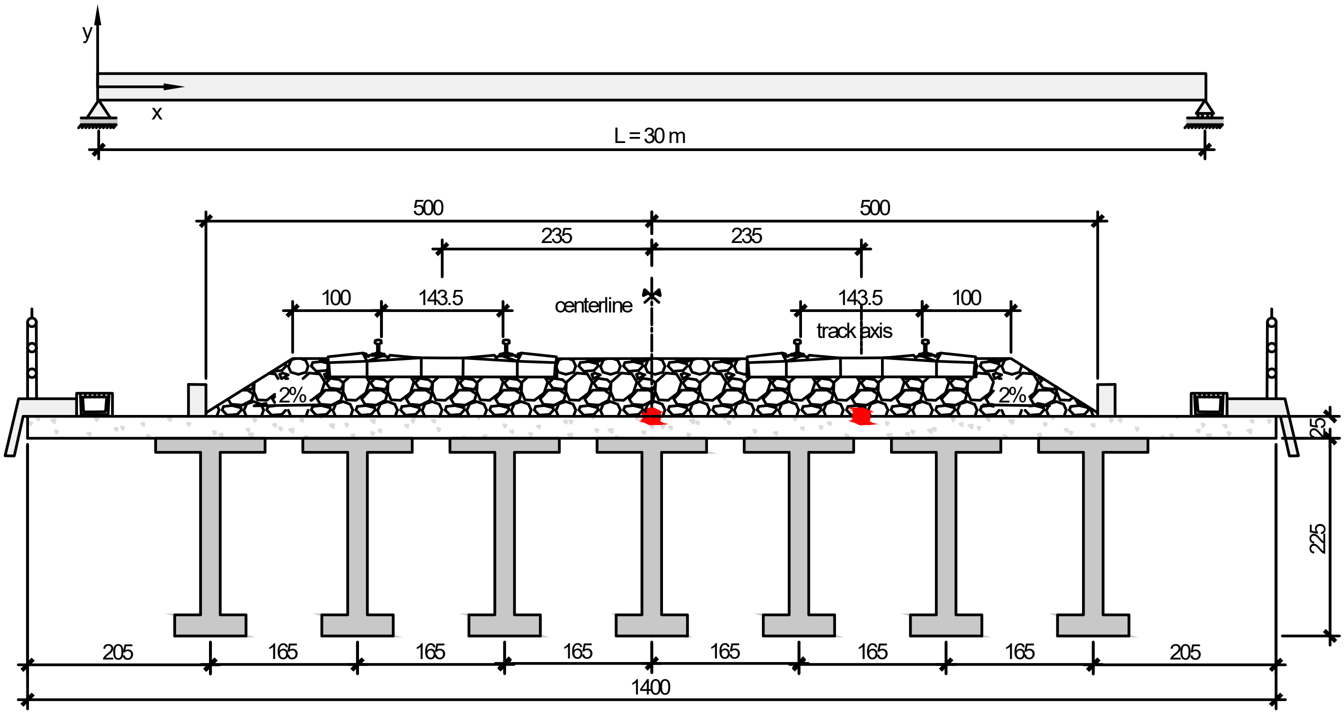

Fig. 3. I-beam cross-section of bridge deck for the case study

All bridge configurations had a span length of 30 m and a total deck depth of 2.50 m, giving a span-to-depth ratio of L/12. The models were treated as simply supported systems and analysed using the same material properties, support idealisation, track arrangement, loading scheme and train speed range. However, the adopted geometry does not represent an optimised design for each bridge type. Instead, it provides a common reference framework for examining how the structural configuration modifies the distribution of mass and stiffness, and consequently the global dynamic response. Fig. 3 shows the cross-sectional layouts and main geometric dimensions used for the I-girder bridge models. The bridge deck models were developed in Abaqus using element formulations selected to reproduce the principal topology of each deck system. The elastic modulus, Poisson's ratio and concrete density were set to 35 GPa, 0.25 and 2500 kg/m³ respectively.

The deck slab of the I-girder bridge was modelled using 10,200 S4R5 reduced-integration shell elements, and the main girders were represented by 1,050 B31 beam elements. Shared nodes were used between the girders and the slab to model composite action. For the U-girder bridge, both the deck slab and the U-girders were represented by 19,200 S4R5 shell elements with tie constraints adopted at their interfaces. The hollow slab and box-girder bridges were modelled using eight-node solid elements. The hollow slab bridge contained 79,050 C3D8R elements and the box-girder bridge contained 38,550 C3D8I elements. A nominal mesh size of 0.2 m was maintained for all bridge configurations.

Different element formulations were selected to reproduce the geometry and load-transfer mechanism of each bridge type. This comparison focuses on global modal properties, vertical displacement and vertical acceleration responses, and is not intended to compare local stress fields between different element formulations. A single HSLM-A1 load model was applied to one track only. The load path was eccentrically positioned with respect to the centreline of the bridge in order to activate both vertical bending and torsional responses in the cross section. This eccentricity was maintained for all configurations to enable the differences in response to be attributed to the combined effects of structural configuration and skewness under a common excitation condition.

3.2. Baseline modal characteristics of straight bridge configurations

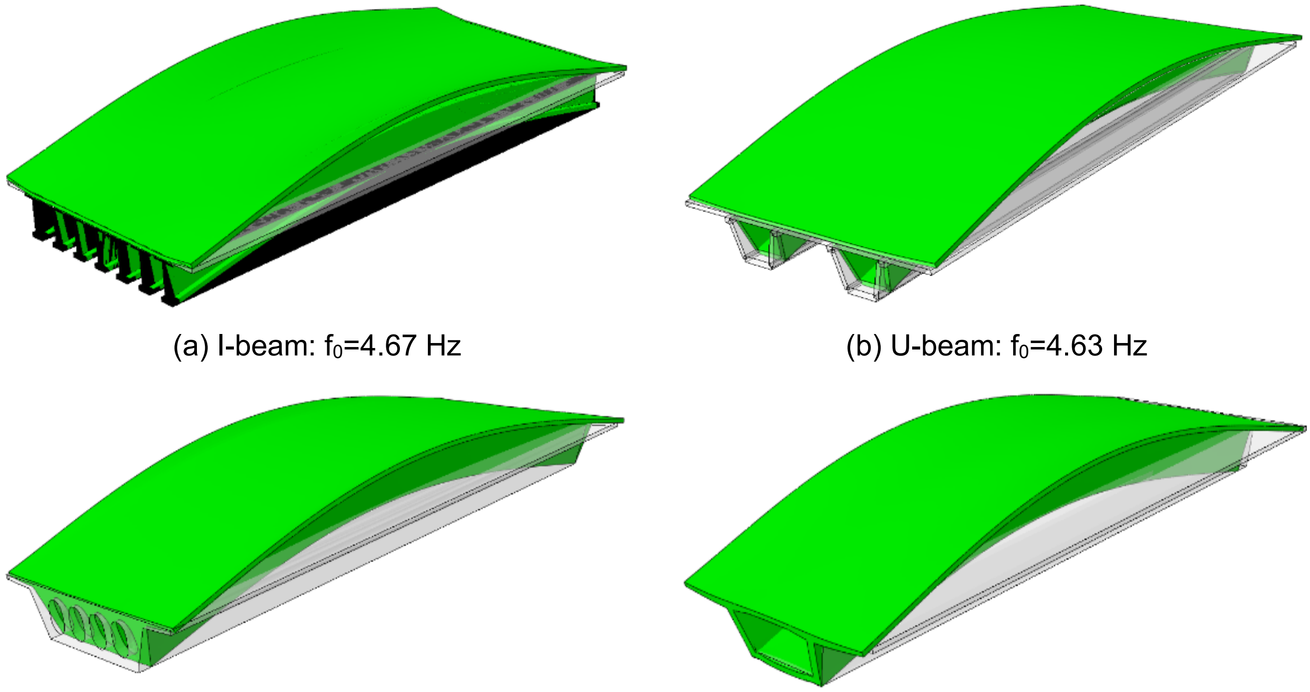

(a) I-beam: f_0=4.67 Hz (b) U-beam: f_0=4.63 Hz

(c) Hollow-slab: f_0=4.67 Hz (d) Box girder: f_0=4.67 Hz

Fig. 4. First bending mode shape of different sections with FE model

A modal analysis was first performed on the straight bridge configurations to establish a common baseline, before the effects of skewness were examined. Fig. 4 shows the first vertical bending mode shapes of the four investigated bridge types. The corresponding frequencies are closely grouped: 4.67 Hz for the I-girder bridge; 4.63 Hz for the U-girder bridge; 4.67 Hz for the hollow slab bridge; and 4.67 Hz for the box-girder bridge. This narrow range of frequencies is important for interpreting the subsequent results. This indicates that any pronounced difference in the speed-dependent response cannot be attributed solely to a substantial difference in the first bending frequency. Instead, the response should be interpreted in relation to the complete structural configuration, including the distribution of stiffness across the deck width, the torsional restraint provided by the cross-section, the eccentricity of the loading path and the modal deformation pattern.

4. Results and discussions

4.1. Dynamic response of straight bridge configurations

Figs. 5 and 6 are used together to evaluate the response of straight bridge configurations under HSLM-A1 loading. Fig. 5 shows typical time histories of vertical displacement and acceleration at the centre of the bridge (CDT) and at the position of the loaded track (CDV), for a train speed of 300 km/h. These histories demonstrate how the response develops over time and how eccentric loading influences the distribution of the response across the deck width. However, they should not be used independently to rank the bridge configurations, as the governing response may occur at a different train speed for each bridge type.

Fig. 6 provides the basis for comparing the speed-dependent responses of the four bridge configurations. Within the investigated speed range, the hollow slab bridge exhibits the lowest levels of displacement and acceleration, while the I-girder and U-girder bridges demonstrate similar response ranges. The box-girder bridge displays an intermediate response. As the first vertical bending frequencies are closely grouped, these differences cannot be interpreted from the first bending mode alone. The cross-sectional configuration, transverse load distribution, torsional response and eccentricity of the moving load must also be considered.

All four straight bridge configurations exhibit a principal resonance region near 300 km/h. For a bridge dominated by vertical bending, the resonance velocity associated with repeated axle loading can be estimated as follows:

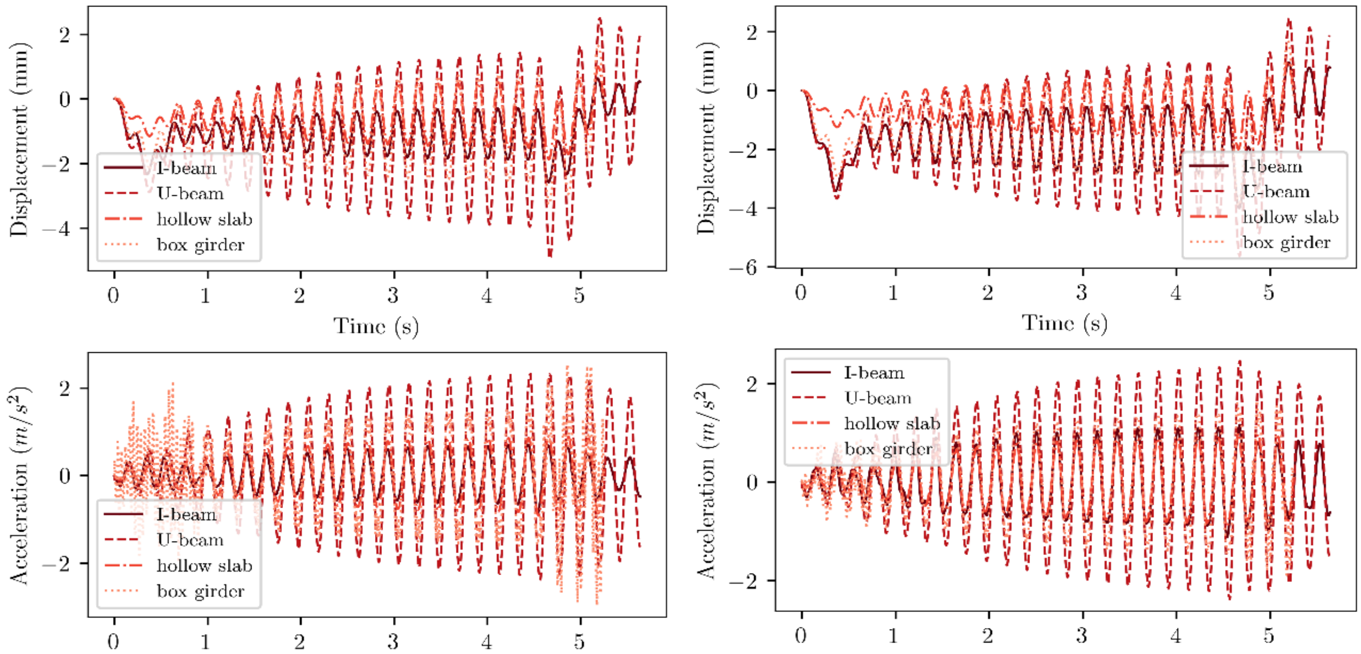

(a) at centerline of section (b) at track axis

Fig. 5. Time histories of vertical displacement and acceleration at the bridge centreline (CDT) and the loaded-track position (CDV) for a train speed of 300 km/h.

$$v_{r,n}=\frac{3.6f_jD}{n} \quad (2)$$

where:

$v_{r,n}$ is the resonance velocity in km/h associated with resonance order (n);

f_j is the natural frequency of the relevant vibration mode in Hz;

D is the characteristic repeated axle spacing in metres;

For the HSLM-A1 loading adopted in this study, D = 18 metres.

Using the first vertical bending frequency of approximately 4.67 Hz, Eq. (2) yields an estimate of the first-order resonance of approximately 303 km/h, which is consistent with the primary response region depicted in Fig. 6.

The I-girder bridge also exhibits a secondary local response peak. This feature should be interpreted in conjunction with the torsion-dominated mode. Under the adopted eccentric loading condition, the secondary peak is consistent with the excitation of this mode, as well as with the

I-girder bridge's greater sensitivity to cross-sectional torsional response. However, this result should not be generalised as evidence that torsional stiffness alone governs the response of all bridge configurations.

4.2 Spatial variation of dynamic response across the deck

Fig. 7 compares the peak responses recorded at the centre of the bridge (CDT) and at the position of the loaded track (CDV). The difference between these two locations reflects the extent to which the deck undergoes cross-sectional rotation and non-uniform transverse deformation when subjected to an eccentrically applied train load. As the load path is offset from the centreline of the bridge, each axle generates a vertical force and a torsional moment about the longitudinal axis of the deck. The resulting response distribution therefore depends on the cross-section's ability to transfer this torsional action through its longitudinal members, slab, webs, and transverse load paths.

The I-girder bridge exhibits the largest difference between CDT and CDV. In this configuration, the train load is primarily transmitted through the deck slab and the girders located near the loaded track. The separated longitudinal load paths and the relatively open cross-sectional arrangement permit a larger rotational component of the deck response. Consequently, the vertical response at the CDV location is more pronounced than at the centre of the bridge, particularly near resonance, when the bending and torsional components of the response are amplified simultaneously.

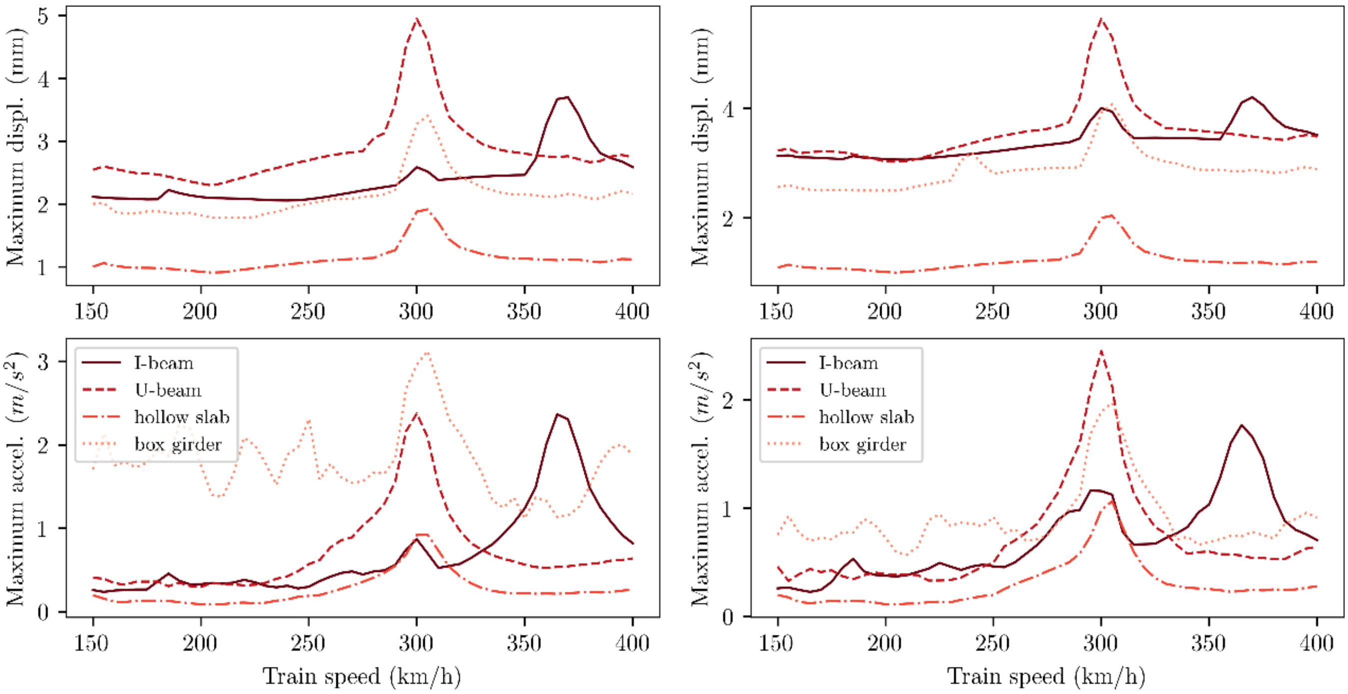

(a) at centerline of section (b) at track axis

Fig. 6. Maximum vertical displacement and acceleration envelopes versus train speed for the investigated straight bridge configurations

The hollow slab bridge exhibits the smallest difference between the two monitoring locations. Its cellular configuration provides continuous load-transfer paths across the deck's entire width, enabling the eccentric load to be redistributed through the webs and top slab before reaching the supports. This mechanism restrains cross-sectional rotation and produces a more uniform vertical response. The box-girder bridge also benefits from torsional continuity due to its closed section. However, local differences in acceleration may still arise near resonance because acceleration is governed not only by global deck rotation, but also by local curvature and modal participation at the monitoring point.

The U-girder bridge exhibits an intermediate response. While its webs and deck slab provide a more continuous transverse load path than the I-girder system, the open upper geometry is more susceptible to transverse deformation than closed hollow slab and box-girder sections. The response pattern therefore reflects a balance between transverse load redistribution and cross-sectional rotational flexibility.

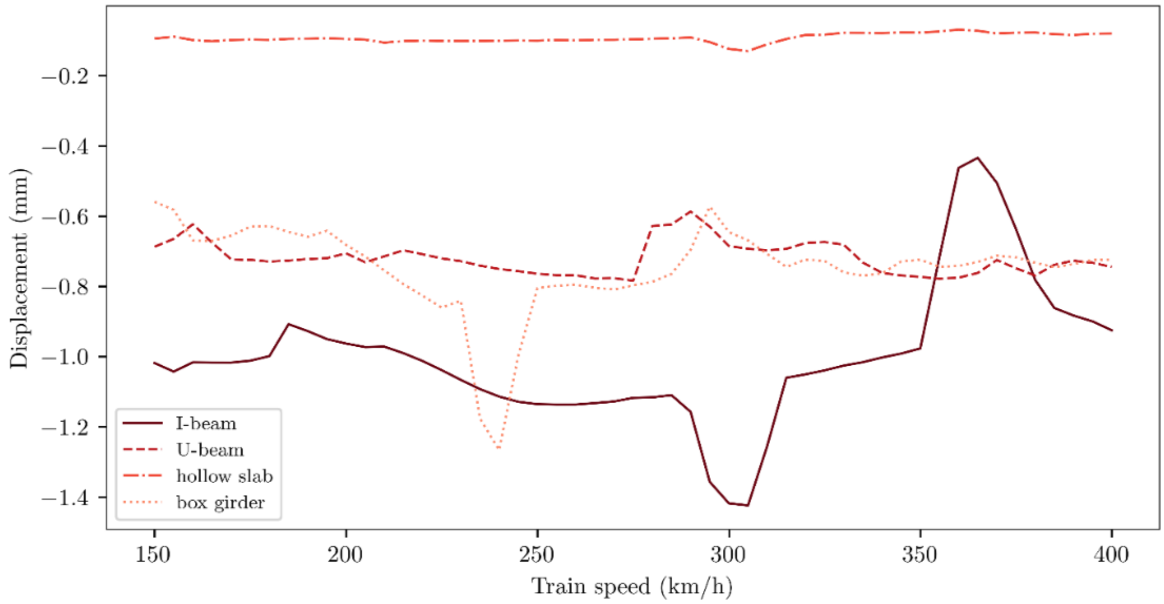

(a) displacement

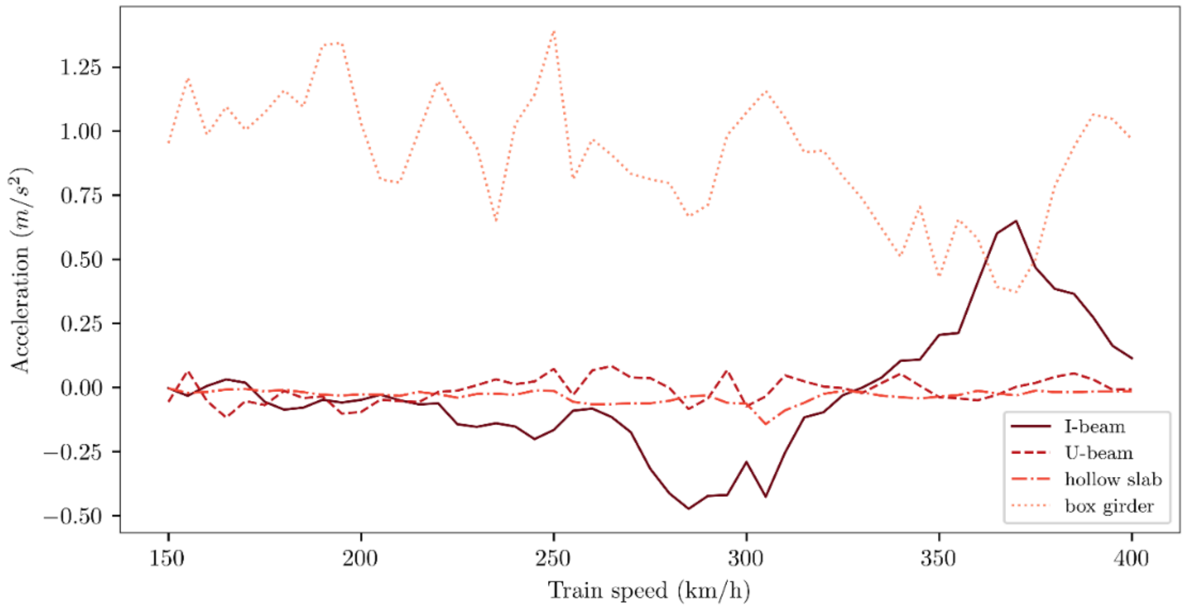

(b) acceleration

Fig. 7. Difference between peak responses at the bridge centreline (CDT) and the loaded-track position (CDV).

These findings are consistent with the broader observation that cross-sectional deformation and torsional participation can influence the response of railway bridges at resonance [24]. They also align with the conclusions of Nguyen [25], who demonstrated that simplified beam representations become less informative when skewness and torsional deformation materially contribute to the global response. In the present study, comparing CDT and CDV provides a direct numerical indication of this effect and identifies the loaded-track position as an essential location for monitoring in subsequent skew-bridge analyses.

4.3. Influence of skew angle

4.3.1. Effect of skew angle on the baseline modal characteristics

In this study, the skew angle is defined as the angle between the support line and the line perpendicular to the longitudinal bridge axis at the support location. Increasing the skew angle modifies the geometry through which the deck is restrained at the supports. For a straight bridge, the support line is perpendicular to the longitudinal axis, meaning that the first vertical mode is predominantly governed by longitudinal bending. In contrast, for a skew bridge, the support condition is imposed along an oblique line, resulting in the deformation of one edge of the deck being coupled with the deformation of the opposite edge. This geometric constraint introduces a flexural–torsional component into the modal deformation, modifying the effective modal stiffness.

Fig. 8 shows that the first vertical bending frequency increases with the skew angle for all the investigated bridge configurations. The I-girder bridge frequency increases by approximately 1.5%, from 4.665 Hz to 4.734 Hz, whereas the hollow slab bridge frequency increases by approximately 22.5%, from 4.674 Hz to 5.724 Hz. The U-girder and box-girder bridges show intermediate increases of around 4.0% and 5.2% respectively.

The pronounced increase in frequency of the hollow slab bridge can be attributed to the interaction between its cellular cross-section and the skew support geometry. The continuous top slab and the internal webs enable a greater proportion of the deck width to contribute to the transfer of support reactions. As the degree of skewness increases, this transverse continuity provides additional restraint against the combined bending and torsion deformation of the deck, thereby increasing the effective modal stiffness.

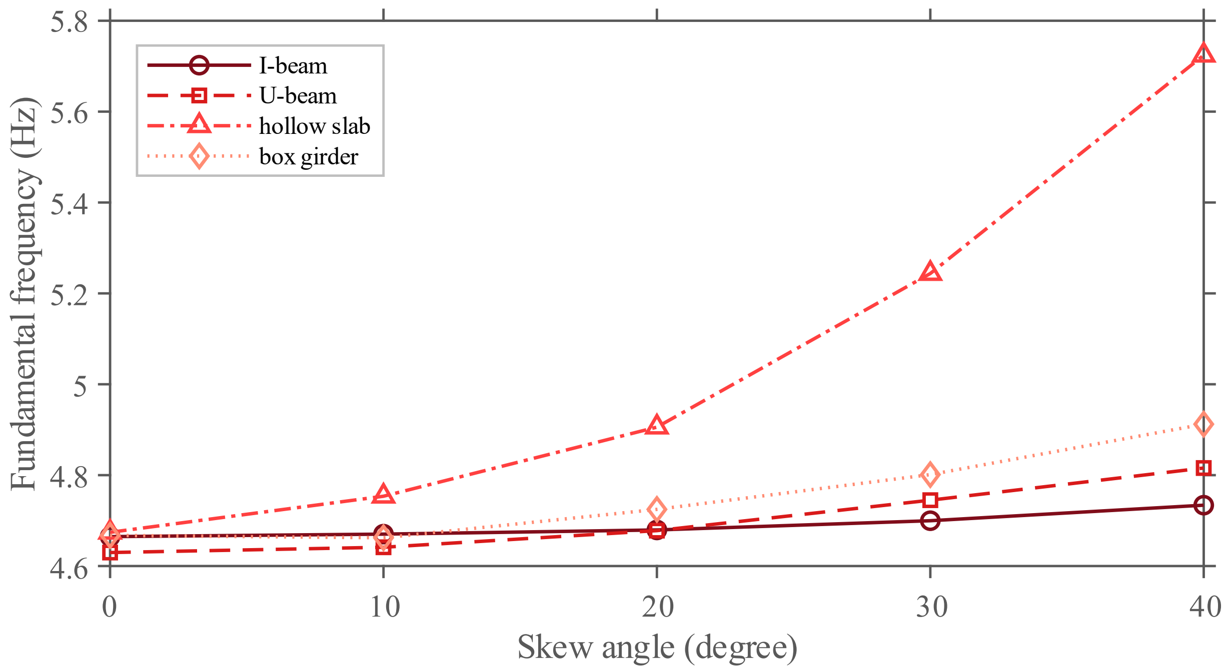

Fig. 8. Variation of the first vertical bending frequency with skew angle

In contrast, the I-girder bridge experiences only a limited increase in frequency. Its response is governed by a system of longitudinal girders connected through the deck slab, and support-induced deformation is partly accommodated through differential bending of the girders and cross-sectional rotation. The resulting increase in effective vertical modal stiffness is therefore smaller than that observed for the hollow slab bridge.

U-girder and box-girder bridges lie between these two extremes. The U-girder develops transverse interaction through its webs and slab, while the box girder benefits from the torsional continuity of its closed section. Their frequency changes suggest that the effect of skewness is due to the combined influence of deck topology, transverse stiffness distribution and support geometry rather than a single stiffness parameter.

4.3.2. Effect of skew angle on displacement and acceleration response envelopes

Figs. 9–12 demonstrate that the position and magnitude of the dynamic-response peaks are both modified by skewness. The shift in the resonance region is a direct consequence of the increase in the relevant modal frequency. For a fixed axle spacing and resonance order, Eq. (2) establishes a proportional relationship between resonance velocity and modal frequency. Consequently, the hollow slab bridge, which exhibits the largest frequency increase, also shows the greatest migration of the principal resonance region towards higher train speeds. The I-girder bridge, for which the first bending frequency changes only slightly, shows a correspondingly limited shift.

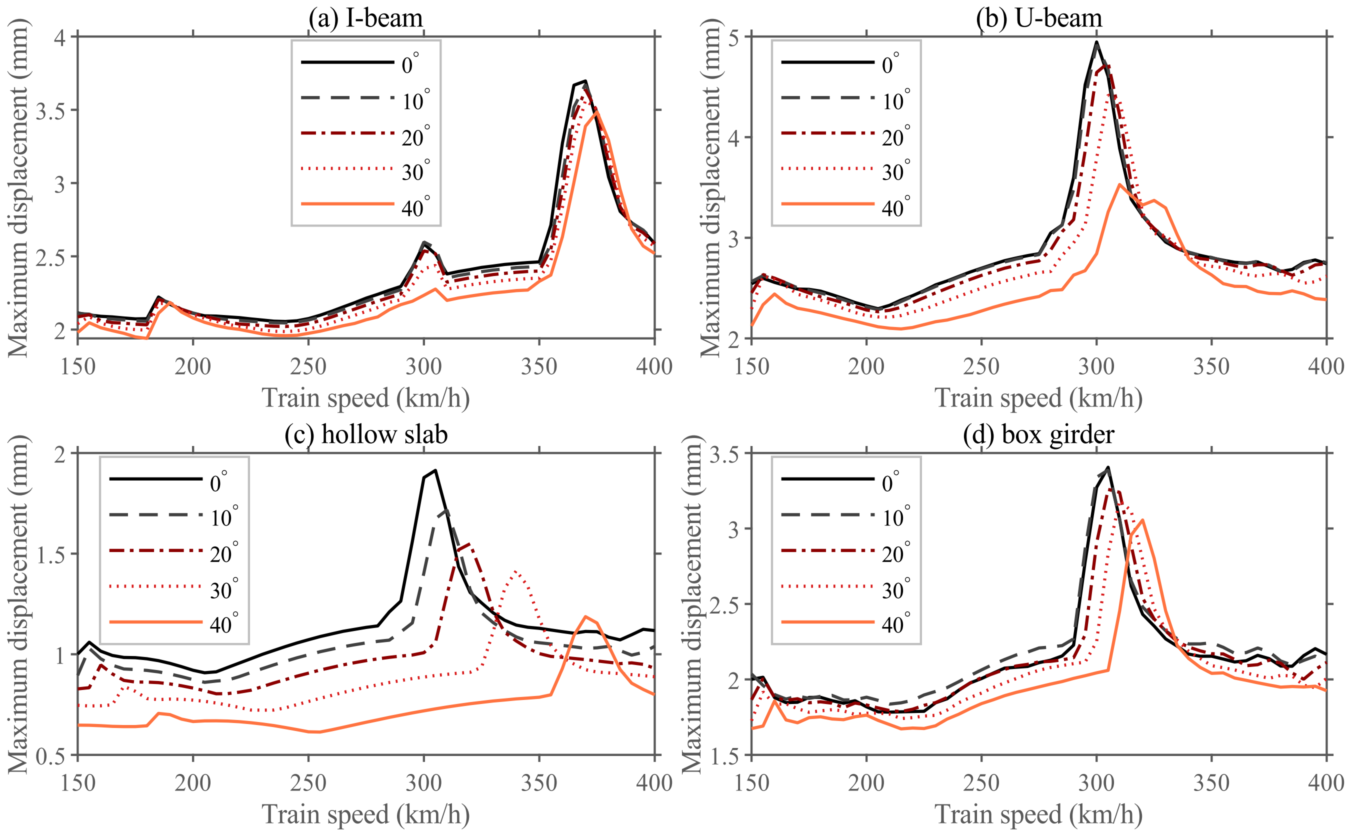

Fig. 9. Maximum vertical displacement envelopes at the bridge centreline (CDT) for different skew angles

The peak magnitude is governed by a more complex mechanism than resonance velocity. This depends on the modal participation factor, the spatial relationship between the moving load and the modal deformation, the damping ratio and the degree to which the response at the selected monitoring location is amplified by cross-sectional rotation. Consequently, the response amplitude does not necessarily vary in direct proportion to the frequency increase.

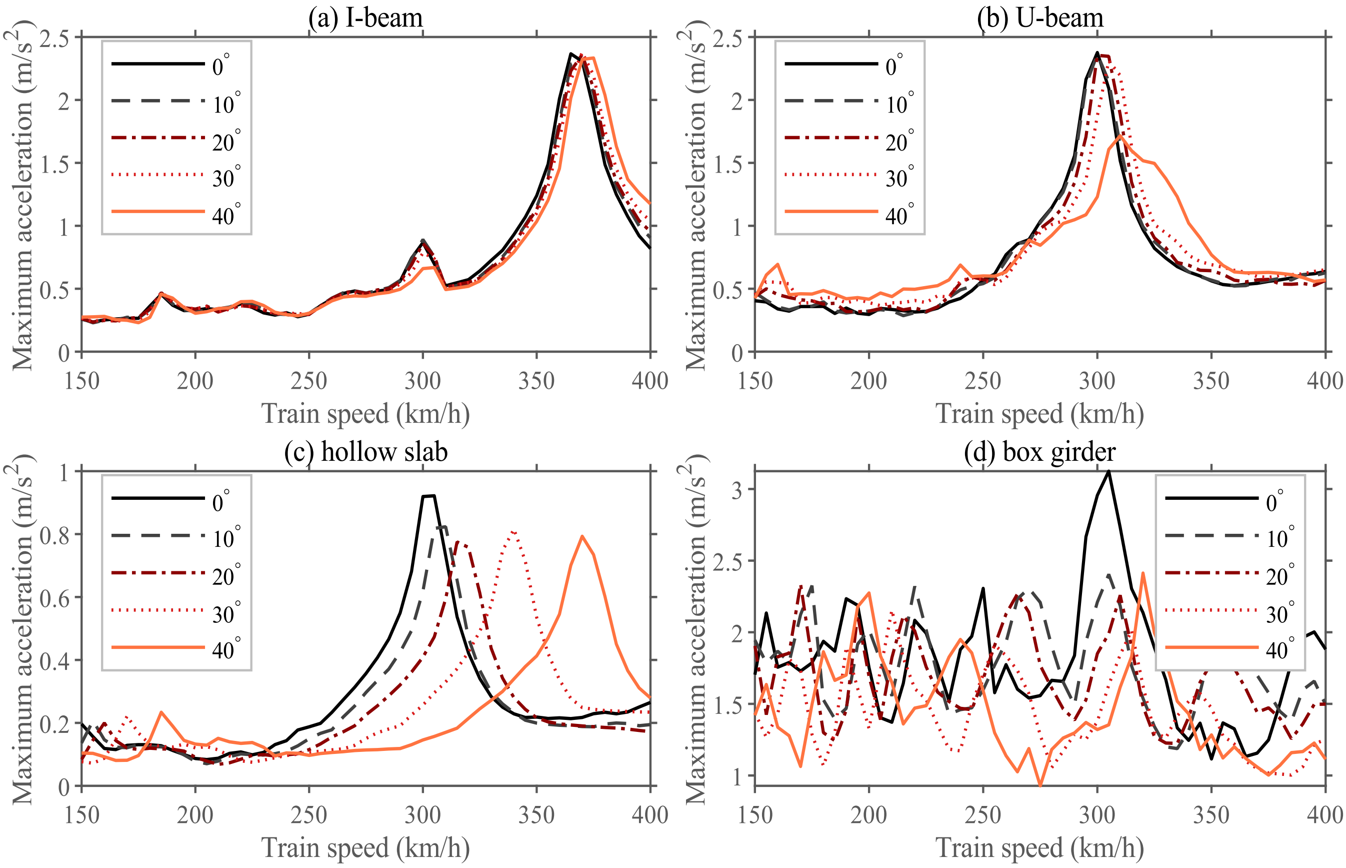

Fig. 10. Maximum vertical acceleration envelopes at the bridge centreline (CDT) for different skew angles

For the I-girder bridge, the response curves remain relatively close together before the main resonance region because the modal properties only vary modestly with the skew angle. The secondary local peak is still evident because the eccentric loading continues to excite the torsion-sensitive deformation of the deck. Therefore, the influence of skewness is primarily expressed through changes in the interaction between closely spaced response components, rather than through substantial displacement of the principal bending resonance. The U-girder bridge shows a more pronounced change in peak magnitude. Its webs and deck slab provide a transverse load-transfer mechanism that becomes increasingly engaged as the skew support condition alters the modal deformation pattern. The resulting changes are most visible near resonance, where the distribution of the moving-load-induced generalised force among the participating modes becomes critical. The hollow slab bridge exhibits the clearest displacement of the resonance region. Its continuous cellular section converts an increasing skew angle into a substantial change in modal stiffness, producing a significant shift in displacement and acceleration envelopes. The box-girder bridge shows intermediate behaviour: its closed section effectively restrains global torsional deformation, while the distribution of mass and stiffness across the deck permits some influence of skewness on the resonance region. The distinction between displacement and acceleration responses is noteworthy. In the study by Nguyen et al. [25], it was found that skewness had a stronger influence on vertical displacement than on maximum acceleration for the considered beam-type bridge configurations. The present results follow the same general pattern for several cases: the resonance location and displacement envelope exhibit a systematic shift with skew angle, whereas acceleration amplitudes are more sensitive to the local modal shape and the selected monitoring position. A fully three-dimensional comparison further shows that this relationship varies with deck typology, particularly when the load is applied eccentrically. All calculated accelerations remain below 3.5 m/s² for the cases investigated. This provides a useful response benchmark within the adopted moving-load framework. However, the assessment is confined to the linear-elastic bridge response because the numerical model does not include vehicle suspension, wheel–rail contact, track irregularity or train–track–bridge interaction.

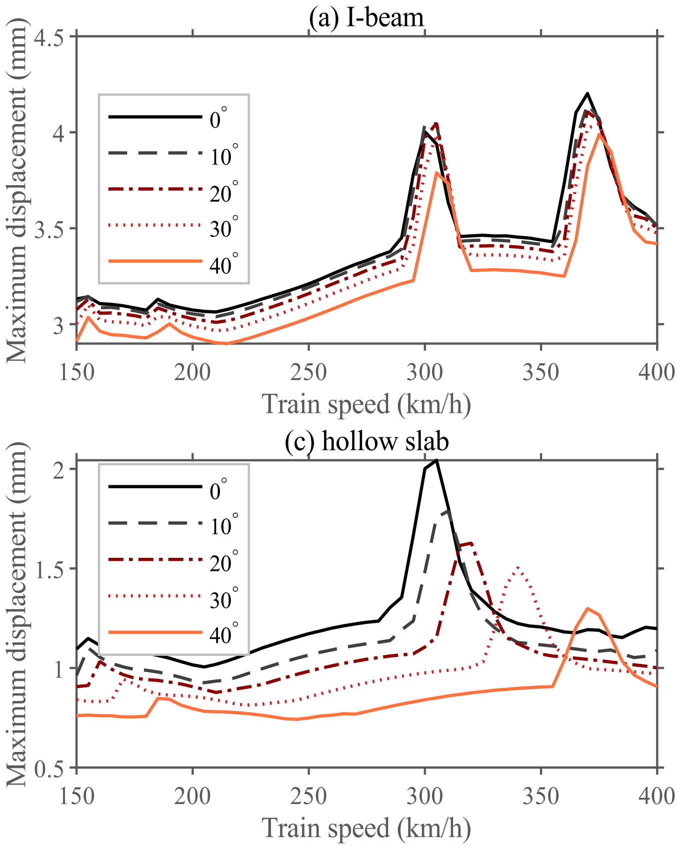

Fig. 11. Maximum vertical displacement envelopes at the loaded-track position (CDV) for different skew angles.

4.3.3. Effect of skew angle on primary resonance velocity

To ensure consistency, the primary resonance velocities shown in Fig. 13 are defined as the train speeds corresponding to the maximum vertical displacement and acceleration at CDV and CDT. This definition uses the same response quantity and monitoring location for all bridge configurations and skew angles, thus avoiding ambiguity when displacement and acceleration peaks occur at slightly different speeds. Fig. 13 follows the modal trend identified in Fig. 8. The hollow slab bridge exhibits the largest increase in primary resonance velocity because its first bending frequency is the most sensitive to the skew support condition. The I-girder bridge shows the least change because its baseline modal frequency is only weakly affected by skewness. The U-girder and box-girder bridges occupy an intermediate position again.

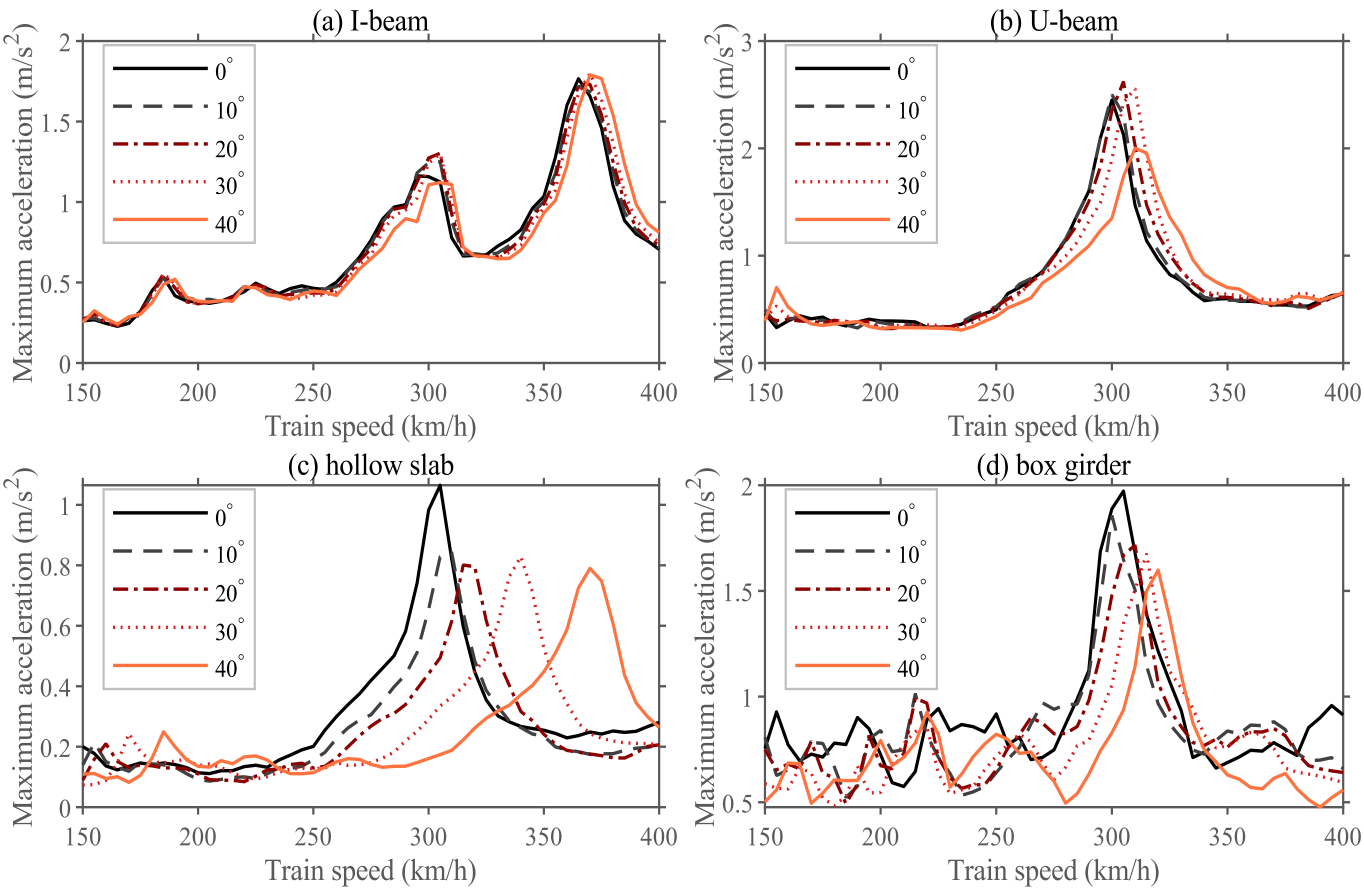

Fig. 12. Maximum vertical acceleration envelopes at the loaded-track position (CDV) for different skew angles

In cases where the same modal component governs the principal response peak, the increase in resonance velocity is expected to follow the increase in the associated modal frequency approximately, as indicated by Eq. (2). However, deviations from this proportional relationship can arise when skewness alters the modal deformation pattern, changes the contribution of torsional components or modifies the spatial relationship between the moving load and the governing mode. In such cases, the resonance peak is determined by the combined modal response of the deck rather than by the first bending frequency alone.

This interpretation provides a more balanced comparison with previous study. Nguyen et al. [25] found that the conventional critical-speed criterion is still useful as a first-order approximation for simply supported skew bridges. They also found that skewness and torsional stiffness become increasingly relevant as the skew angle increases. The present study corroborates this general conclusion while demonstrating that the magnitude of the resonance shift varies significantly among I-girder, U-girder, hollow slab and box-girder decks. A recent study by Phung et al. [26] on hollow slabs similarly attributes the response of skew railway bridges to coupled flexural–torsional modes rather than a purely planar bending mechanism.

4.4. Synthesis and implications for preliminary modelling

The preceding results demonstrate that the configuration of a bridge's cross section affects its dynamic response through a set of interacting mechanisms rather than a single parameter. While the first vertical bending frequency establishes the approximate resonance region, the magnitude and spatial distribution of the response are governed by the combined effects of cross-sectional topology, transverse load-transfer capacity, torsional restraint, modal deformation pattern, eccentric loading and support geometry.

Comparing the four bridge configurations shows that similar first bending frequencies do not necessarily result in similar dynamic responses. The straight I-girder, U-girder, hollow slab and box-girder bridges have closely grouped initial vertical frequencies, yet their response envelopes and cross-sectional response distributions differ substantially. This is because the same global bending frequency can be associated with different modal shapes and capacities for redistributing an eccentric train load across the deck width.

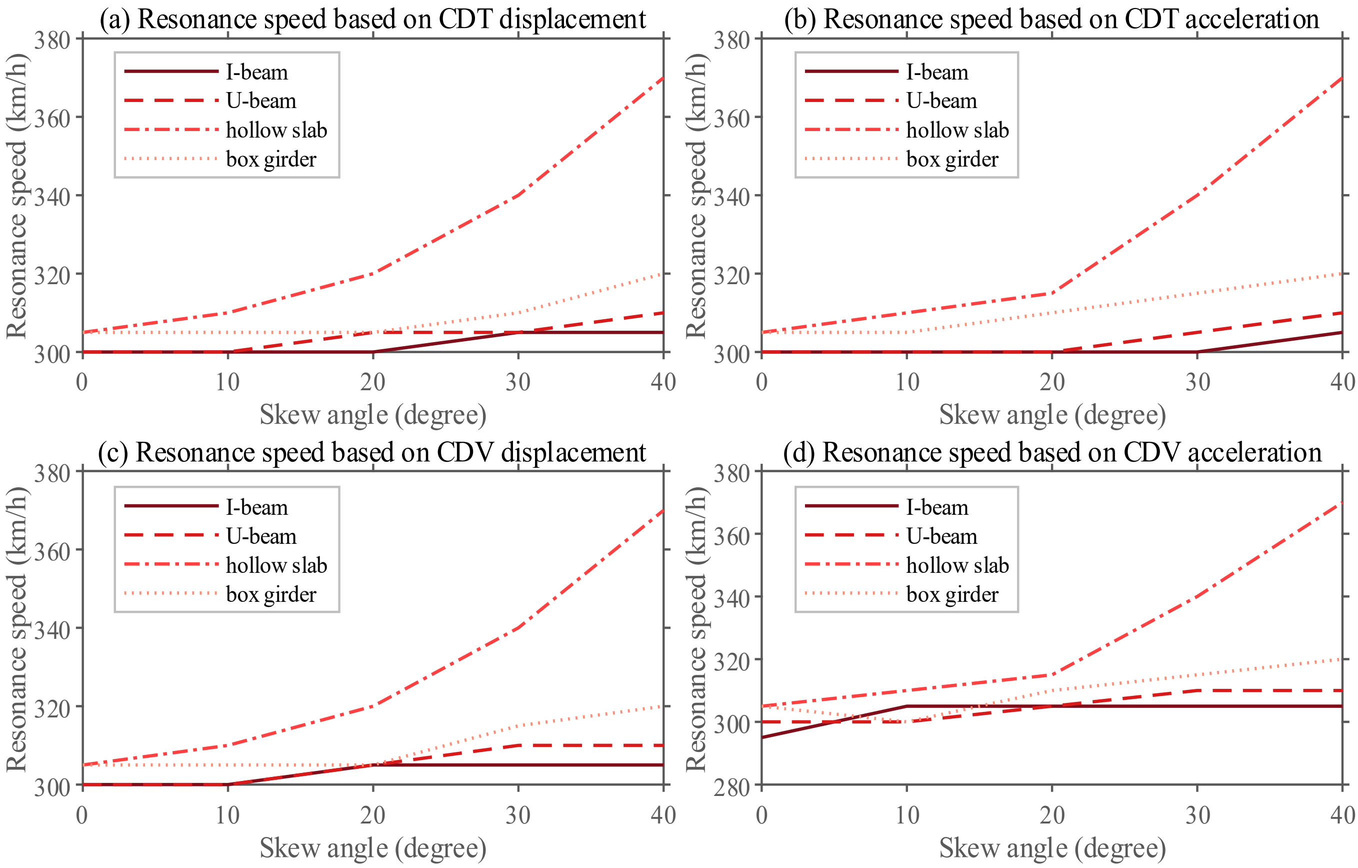

Fig. 13. Relationship between resonance velocity and skew angle

The influence of skewness further amplifies these distinctions. For the hollow slab bridge, the cellular deck and skew support geometry interact to increase modal stiffness and significantly shift the resonance region. In contrast, for the I-girder bridge, a smaller change in the first bending frequency is accompanied by a more significant impact of cross-sectional rotation and a more sensitive response to torsion. The U-girder and box-girder bridges exhibit intermediate behaviour due to their structural arrangements providing partial restraint against deformation induced by eccentric loading and skew supports, but not identical restraint.

These results provide a basis for selecting the appropriate modelling level during a preliminary dynamic assessment. A beam-based model can efficiently provide an initial estimate when the bridge is straight, the response is primarily global vertical bending and remains relatively uniform across the deck width. A three-dimensional model is more informative when the deck exhibits pronounced differences in response between the bridge centreline and the loaded track, when the skewness of the bridge substantially changes the modal characteristics, or when the response near resonance is significantly affected by torsion-sensitive modes. This distinction is consistent with the earlier observation that local and cross-sectional deformation may become relevant at resonance, particularly for structural systems in which the load path and modal deformation cannot be adequately represented by a single planar beam.

However, the conclusions are limited to the linear-elastic moving-load framework adopted in this study. While they provide comparative evidence for bridge modelling and preliminary dynamic interpretation, detailed serviceability or running-safety assessment requires additional consideration of train–track–bridge interaction and track-related effects.

5. Conclusions

This study compared the dynamic response of four 30 m simply supported high-speed railway bridge configurations within the same HSLM-A1 moving-load framework. The main findings are as follows:

(1) The first vertical bending frequencies of straight bridges are closely grouped between 4.63 and 4.67 Hz. However, their speed-dependent displacement and acceleration responses differ substantially. Therefore, the dynamic behaviour is governed by the complete structural configuration, including the transverse load path, cross-sectional stiffness distribution, modal deformation pattern and loading eccentricity.

(2) The I-girder bridge exhibits the largest difference between the bridge centreline and the loaded-track position, indicating a stronger contribution of cross-sectional rotation under eccentric loading. The hollow slab bridge exhibits the most uniform response across the deck width because its cellular configuration provides continuous transverse load-transfer paths.

(3) Increasing the skew angle modifies the modal stiffness of all bridge configurations. As the skew angle increases from 0° to 40°, the first vertical bending frequency increases by approximately 1.5% for the I-girder bridge, 4.0% for the U-girder bridge, 5.2% for the box-girder bridge and 22.5% for the hollow slab bridge.

(4) As skewness increases, the resonance region shifts towards higher train speeds. The magnitude of this shift is proportional to the configuration-dependent change in modal frequency, being largest for the hollow slab bridge. The resonance response is also affected by modal participation, cross-sectional rotation and the spatial relationship between the moving load and the governing mode.

(5) The results show that, while the first bending frequency remains a useful preliminary indicator of the resonance region, a three-dimensional model provides additional value when appreciable variation across the deck width is produced by skewness, eccentric loading, or cross-sectional torsional response. These findings apply to the adopted linear-elastic moving-load model and are intended for comparative modelling and preliminary dynamic assessment.

Declaration of Generative AI

During the preparation of this work, the authors do not use Generative AI and AI-assisted technologies tools in order to generate the content of the manuscript.

References

[1]. International Union of Railways. (2023) UIC: High-Speed around the world.

[2]. J. Campos, G. de Rus. (2009). Some stylized facts about high-speed rail: A review of HSR experiences around the world. Transport Policy, 16(1), 19–28. https://doi.org/10.1016/j.tranpol.2009.02.008

[3]. TEDI–TRICC–TEDISOUTH Consulting Joint Venture. (2024). Pre-Feasibility Study Report for the North–South High-Speed Railway Project (in Vietnamese).

[4]. B. Yan, G.-L. Dai, N. Hu. (2015). Recent development of design and construction of

short span high-speed railway bridges in China. *Engineering Structures*, 100, 707–717. https://doi.org/10.1016/j.engstruct.2015.06.050

[5]. B. Bachinilla, A. Evangelista, M. Siddhpura, A.N. Haddad, B.B.F. da Costa. (2022). High-Speed Railway Bridge and Pile Foundation: A Review. *Infrastructures*, 7(11), 154. https://doi.org/10.3390/infrastructures7110154

[6]. European Committee for Standardization (CEN). (2023). EN 1991-2 (2023): Eurocode 1: Actions on structure - Part 2: Traffic loads on bridges and other civil engineering works.

[7]. Ministry of Railways of the People's Republic of China. (2014). TB 10621–2014 Code for Design of High-speed Railway Bridges.

[8]. Railway Technical Research Institute. (2012). Design Standards for Railway Structures and Commentary: Bridges.

[9]. Ministry of Science and Technology. (2022). TCVN 13594:2022 Railway Bridge Design with gauge 1435 mm, speed up to 350 km/h (in Vietnamese).

[10]. R. Hibbeler. (2022). Mechanics of Materials. *Pearson*.

[11]. J.M. Gere, B.J. Goodno. (2011). Mechanics of Materials, Brief Edition. *Cengage Learning.*

[12]. S. Timoshenko, J.N. Goodier. (1970). Theory of Elasticity, 3rd ed. McGraw-Hill.

[13]. R.W. Clough, J. Penzien. (1993). Dynamics of Structures. *McGraw-Hill.*

[14]. A.K. Chopra. (2017). Dynamics of Structures: Theory and Applications to Earthquake Engineering. *Pearson*.

[15]. L. Frýba. (1996). Dynamics of Railway Bridges. *Thomas Telford.*

[16]. W. Zhai, H. Xia, C. Cai, M. Gao, X. Li, X. Guo, N. Zhang, K. Wang. (2013). High-speed train–track–bridge dynamic interactions – Part I: theoretical model and numerical simulation. *International Journal of Rail Transportation*, 1(1-2), 3–24. https://doi.org/10.1080/23248378.2013.791498

[17]. H. Xia, N. Zhang, W. Guo. (2018). Dynamic Interaction of Train-Bridge Systems in High-Speed Railways: Theory and Applications. *Springer*. https://doi.org/10.1007/978-3-662-54871-4

[18]. Y.B. Yang, J.D. Yau, Y.S. Wu. (2004). Vehicle–Bridge Interaction Dynamics: With Applications to High-Speed Railways. https://doi.org/10.1142/5541

[19]. W. Zhai, Z. Han, Z. Chen, L. Ling, S. Zhu. (2019). Train–track–bridge dynamic interaction: a state-of-the-art review. *Vehicle System Dynamics*, 57(7), 984–1027. https://doi.org/10.1080/00423114.2019.1605085

[20]. W.-F. Chen, L. Duan. (2014). Bridge Engineering Handbook: Substructure Design. *CRC Press*. https://doi.org/10.1201/b15621

[21]. J. Romo, A. Perez-Caldentey, M. Cuadrado. (2023). High-speed Railway Bridges: Conceptual Design Guide. *Wiley*.

[22]. L. Zhu, H.-L. Wang, B. Han, G.-Y. Zhao, X.-J. Huo, X.-Z. Ren. (2020). Dynamic analysis of a coupled steel-concrete composite box girder bridge-train system considering slip and shear-lag. *Thin-Walled Structures*, 157, 107060. https://doi.org/10.1016/j.tws.2020.107060

[23]. R. Bebiano, R. Calçada, D. Camotim, N. Silvestre. (2017). Dynamic analysis of high-speed railway bridge decks using generalised beam theory. *Thin-Walled Structures*, 114, 22–31. https://doi.org/10.1016/j.tws.2017.01.027

[24]. S.I. Kim, H.M. Kim, I.H. Yeo. (2010). A study on the comparison of dynamic behaviour of high speed railway bridges. Presented at the Structures Under Shock and Impact XI (SUSI), pp. 159-169. doi: 10.2495/SU100141

[25]. K. Nguyen, C. Velarde, J.M. Goicolea. (2019). Analytical and simplified models for dynamic analysis of short skew bridges under

moving loads. *Advances in Structural Engineering*, 22(9), 2076–2088. https://doi.org/10.1177/1369433219831481

[26]. T.B. Phung, D.X. Nguyen, V.K. Ly, K. Nguyen. (2026). Dynamic analysis of skew hollow-slab railway bridges under high-speed train loads using three-dimensional finite element and analytical beam models. *Advances in Science and Technology Research Journal*, 20(7), 263–277. https://doi.org/10.12913/22998624/219366

[27]. A. Doménech, P. Museros, M.D. Martínez-Rodrigo. (2014). Influence of the vehicle model on the prediction of the maximum bending response of simply-supported bridges under high-speed railway traffic. *Engineering Structures*, 72, 123–139. https://doi.org/10.1016/j.engstruct.2014.04.037

[28]. E. Moliner, P. Museros, R. Allahvirdizadeh. (2024). Track–bridge interaction effects in the acceleration and displacement response of high-speed railway bridges: Simplified *vs* refined modelling. *Engineering Structures*, 314, 118304. https://doi.org/10.1016/j.engstruct.2024.118304

[29]. Dassault Systèmes. (2024). Abaqus 2024 Documentation. Dassault Systèmes Simulia Corp.